"Wheeling Templates" in Molecular Oxothiomolybdate Rings: Syntheses, Structures, and Dynamics

Bernadette Salignac, Sandra Riedel, Anne Dolbecq, Francis Sécheresse, and Emmanuel Cadot*

Contribution from the Institut Lavoisier, IREM, UMR CNRS 8637, Université de Versailles Saint-Quentin, 45 avenue des Etats-Unis, 78035 Versailles, France

Received May 30, 2000

Abstract: The influence of three dicarboxylate anions, oxalate, $(C_2O_4)^{2-}$, glutarate, $(H_6C_5O_4)^{2-}$, and pimelate, $(H_{10}C_7O_4)^{2-}$, on the self-condensation process of the $[Mo_2S_2O_2]^{2+}$ dithiocation has been investigated. $[Mo_8S_8O_8(OH)_8(C_2O_4)]^{2-}$ ($[Mo_8\text{-ox}]^{2-}$), $[Mo_{10}S_{10}O_{10}(OH)_{10}(H_6C_5O_4)]^{2-}$ ($[Mo_{10}\text{-glu}]^{2-}$), and $[Mo_{12}S_{12}O_{12}(OH)_{12}(H_{10}C_7O_4)]^{2-}$ ($[Mo_{12}\text{-pim}]^{2-}$) have been prepared and characterized in aqueous solution by ^{1}H NMR and electrospray mass spectroscopy and in the solid state by elemental analyses, X-ray crystallography, and infrared spectroscopy. The molecular arrangement of $[Mo_8\text{-ox}]^{2-}$, $[Mo_{10}\text{-glu}]^{2-}$, and $[Mo_{12}\text{-pim}]^{2-}$ exhibits the same type of topology derived from the neutral cyclic $\{Mo_{2n}S_{2n}O_{2n}(OH)_{2n}\}$ backbone. $\{Mo_{2n}S_{2n}O_{2n}(OH)_{2n}\}$ inorganic rings encapsulate the organic guest with direct covalent interactions between Mo centers and carboxylate groups. Excess of glutarate does not change the molecular arrangement of the anion but modifies the solid-state arrangement of $[Mo_{10}\text{-glu}]^{2-}$. $Rb_4(C_5H_6O_4)[Mo_{10}S_{10}O_{10}(OH)_{10}(H_6C_5O_4)]\cdot 5H_2O$ ($Rb_4glu[Mo_{10}\text{-glu}]\cdot 5H_2O$) has been crystallized and structurally characterized by X-ray diffraction. The structure of $Rb_4glu[Mo_{10}\text{-glu}]\cdot 5H_2O$ contains the same decameric molecular anion as that found in $Cs_2[Mo_{10}\text{-glu}]\cdot 20H_2O$ with an additional glutarate capping the molecular wheel. The supramolecular interactions developed in $Rb_4glu[Mo_{10}\text{-glu}]\cdot 5H_2O$ are ensured by hydrogen bonds involving the hydroxo bridges of the inorganic ring and the carboxylate groups of the additional glutarate. Negative-ion electrospray mass spectroscopy (ESMS) has been performed on aqueous solution containing the $\{Mo_2S_2O_2\}$ building block and the templating agent at pH 4.5. The anions $[Mo_8\text{-ox}]^{2-}$, $[Mo_{10}\text{-glu}]^{2-}$, and $[Mo_{12}\text{-pim}]^{2-}$ were clearly identified by their parent peaks observed in the ESMS spectra. Experimental *m*/*z* ratios are fully consistent with the corresponding X-ray diffraction results. The templated anionic Mo_{2n} rings have been characterized by ^{1}H NMR spectroscopy in aqueous solution and in acetonitrile-d_3. The ^{1}H NMR spectra of $[Mo_8\text{-ox}]^{2-}$, $[Mo_{10}\text{-glu}]^{2-}$, and $[Mo_{12}\text{-pim}]^{2-}$ as Li^+ salts in CD_3CN unambiguously contain the resonances of the hydroxo bridges belonging to the ring and those of the inner CH_2 groups of the alkyl chain in $[Mo_{10}\text{-glu}]^{2-}$ and $[Mo_{12}\text{-pim}]^{2-}$. Variable-temperature ^{1}H NMR spectra recorded in CD_3CN revealed the fluxionality of $[Mo_{10}\text{-glu}]^{2-}$ and $[Mo_{12}\text{-pim}]^{2-}$ in contrast to the rigidity of $[Mo_8\text{-ox}]^{2-}$. At low temperature ($T = 226$ K), the motion of the guest, i.e., the central template in Mo_{10} and Mo_{12} rings, becomes slow enough on the NMR time scale to postulate the presence of conformational isomers in solution.

Introduction

A striking feature of the soluble metal oxide clusters, so-called polyoxometalates, is their ability to incorporate functional organic ligands[1] to mimic the catalytic properties of metal oxide surface or for tailoring specific molecular shapes through host−guest interactions. The templating influence of the organic part on the oxometalate self-condensation was widely demonstrated for solid-state phases built up from infinite or discrete transition metal−oxygen combinations.[2,3] Conversely, metal−sulfur molecular associations appear commonly based on single archetypal structural building blocks with low nuclearity.[4] In a previous work, we reported an elegant way to extend this class of compounds to the Keggin-type structures. The first heteropoly-oxothio compounds γ-$[SiW_{10}M_2S_2O_{38}]^{6-}$ (M = Mo, W) resulted from the stereospecific addition of the $[M_2S_2O_2]^{2+}$ thiocation to the divacant anion γ-$[SiW_{10}O_{36}]^{8-}$.[5] We have extended this method to other polyvacant anions, such as α-$[PW_9O_{34}]^{9-}$.[6] The self-condensation of the reactive $[Mo_2S_2O_2]^{2+}$ precursor was then at the origin of the development of a new subclass of compounds: the cyclic polyoxothiometalates.[7] If the coordination of the dinuclear oxo or oxothio cation $[M_2E_2O_2]^{2+}$ (M = W,

(1) Gouzerh, P.; Proust, A. *Chem. Rev.* **1998**, *98*, 77−111.

(2) (a) Chen, Q.; Zubieta, J. *J. Chem. Soc., Chem. Commun.* **1994**, 2663. (b) Salta, J.; Chen, Q.; Chang, Y. D.; Zubieta, J. *Angew. Chem., Int. Ed. Engl.* **1994**, *33*, 757. (c) Chang, Y. D.; Salta, J.; Zubieta, J. *Angew. Chem., Int. Ed. Engl.* **1994**, *33*, 325. (d) Huan, G. H.; Jacobson, A. J.; Day, V. W. *Angew. Chem., Int. Ed. Engl.* **1991**, *30*, 422. (e) Chen, Q.; Zubieta, J. *J. Chem. Soc., Chem. Commun.* **1994**, 1635. (f) Khan, M. I.; Zubieta, J. *Angew. Chem., Int. Ed. Engl.* **1994**, *33*, 760. (g) Müller, A.; Hovemeier, K.; Rohlfing, R. *Angew. Chem., Int. Ed. Engl.* **1992**, *31*, 1192. (h) Huan, G. H.; Day, V. W.; Jacobson, A. J.; Goshorn, D. P. *J. Am. Chem. Soc.* **1991**, *113*, 3188.

(3) (a) Chen, Q.; Liu, S.; Zubieta, J. *Angew. Chem., Int. Ed. Engl.* **1990**, *29*, 70. (b) Lowe, M. P.; Lockhart, J. C.; Clegg, W.; Fraser, K. A. *Angew. Chem., Int. Ed. Engl.* **1994**, *33*, 451. (c) Cao, G.; Haushalter, R. C.; Strohmaier, K. G. *Inorg. Chem.* **1993**, *32*, 127. (d) Khan, M. I.; Chen, Q.; Zubieta, J. *Inorg. Chim. Acta* **1993**, *206*, 131. (e) Khan, M. I.; Chen, Q.; Zubieta, J. *Inorg. Chim. Acta* **1995**, *231*, 13.

(4) See for a review: Shibahara, T. *Coord. Chem. Rev.* **1993**, *123*, 73−147.

(5) (a) Cadot, E.; Béreau, V.; Halut, S.; Sécheresse, F. *Inorg. Chem.* **1996**, *35*, 551. (b) Cadot, E.; Béreau, V.; Sécheresse, F. *Inorg. Chim. Acta* **1996**, *252*, 101.

(6) Béreau, V.; Cadot, E.; Bögge, H.; Müller, A.; Sécheresse, F. *Inorg. Chem.* **1996**, *35*, 551.

(7) Sécheresse, F.; Cadot, E.; Dolbecq, A. *J. Solid State Chem.* **2000**, *152*, 78.

10.1021/ja001878t CCC: $19.00
Published on Web 10/07/2000

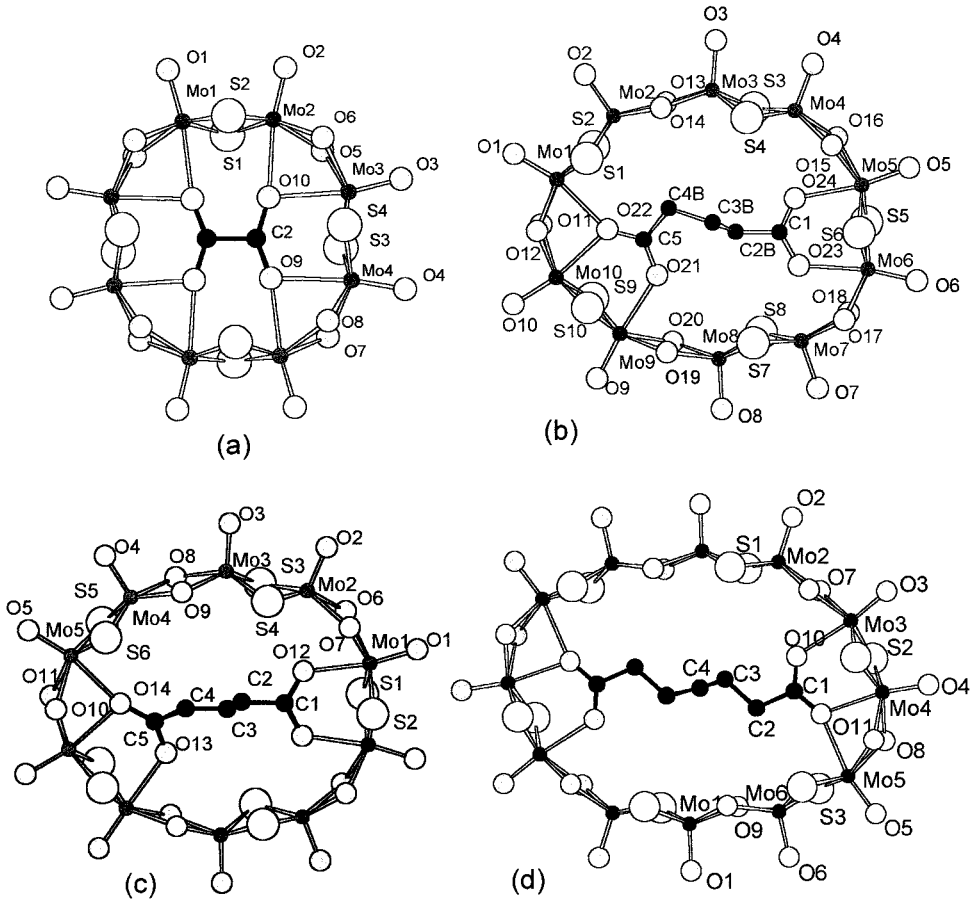

Figure 1. Atom-labeling scheme for the molecular anions $[Mo_8S_8O_8(OH)_8(C_2O_4)]^{2-}$ (a), $[Mo_{10}S_{10}O_{10}(OH)_{10}(H_6C_5O_4)]^{2-}$ in $Cs_2[Mo_{10}\text{-glu}]\cdot 11H_2O$ (b), $[Mo_{10}S_{10}O_{10}(OH)_{10}(H_6C_5O_4)]^{2-}$ in $Rb_4glu[Mo_{10}\text{-glu}]\cdot 5H_2O$ (c), and $[Mo_{12}S_{12}O_{12}(OH)_{12}(H_{10}C_7O_4)]^{2-}$ (d).

Mo; E = O, S) with various organic ligands has been extensively studied,[8] the acidobasic properties has never been investigated. In a previous work, we demonstrated that the $[Mo_2S_2O_2]^{2+}$ dithiocation can act as a Brønsted acid. In the presence of hydroxide ions, the dithiocation rapidly polymerizes to form the neutral dodecameric wheel $[Mo_{12}S_{12}O_{12}(OH)_{12}(H_2O)_6]$.[9] This compound exhibits a ring-shaped architecture with an open central cavity of about 11 Å in diameter. We have recently shown that anionic reagents (HXO_4^{2-}, X = P, As) could be inserted in the open cavity, illustrating the cationic character of the inner ring.[10] Moreover, the inorganic backbone can adapt its nuclearity and geometry to those of the anionic reagent. In $[(HPO_4)_2Mo_{12}S_{12}O_{12}(OH)_{12}(H_2O)_2]^{4-}$, the original circular wheel adopts an elliptical shape, while in $[(H_2XO_4)Mo_{10}S_{10}O_{10}(OH)_{11}(H_2O)_2]^{2-}$, a structural rearrangement is observed. In aqueous solution, the two phosphato compounds are in equilibrium, and their distribution depends on the initial phosphate concentration. In the presence of iodide, the decameric $[Mo_{10}S_{10}O_{10}(OH)_{10}(H_2O)_5]$ ring exhibits a supramolecular arrangement[11] in which the cohesion of the decamer is ensured by two capping iodide ions interacting with the inner water molecules through hydrogen bonding. Metalates such as tetraoxomolybdate, $[MoO_4]^{2-}$, can also act as templates and provide specific mixed-valence compounds. In $[Mo^V_8Mo^{VI}S_8O_{10}(OH)_{10}(H_2O)]^{2-}$, the octameric $\{Mo_8S_8O_8(OH)_8\}$ wheel encapsulates the central octahedron $\{H_4MoO_6\}^{2-}$.[12] We have chosen to study the influence of the linear chain of dicarboxylate anions on the condensation, the goal of the work being to control the nuclearity of the wheel via the length of the alkyl chain of the guest organic anion. Oxalic acid ($H_2C_2O_4$), glutaric acid ($H_8C_5O_4$), and pimelic acid ($H_{12}C_7O_4$) give $[Mo_8S_8O_8(OH)_8(C_2O_4)]^{2-}$ ($[Mo_8\text{-ox}]^{2-}$), $[Mo_{10}S_{10}O_{10}(OH)_{10}(H_6C_5O_4)]^{2-}$ ($[Mo_{10}\text{-glu}]^{2-}$), and $[Mo_{12}S_{12}O_{12}(OH)_{12}(H_{10}C_7O_4)]^{2-}$ ($[Mo_{12}\text{-pim}]^{2-}$), each characterized by X-ray diffraction studies. In solution, electrospray mass spectroscopy experiments (ESMS) provided further evidence of the control of the nuclearity through the characterization of the templated Mo_8, Mo_{10}, and Mo_{12} rings. Variable-temperature ^1H NMR experiments recorded down to 226 K revealed an unusual dynamic flexibility of the Mo_{10} and Mo_{12} inorganic backbones.

Results and Discussion

Structures of the Anions. In Figure 1 are depicted the molecular structures of the Mo_8-, Mo_{10}- and Mo_{12}-templated anions. Crystal data and selected bond lengths are given in Tables 1 and 2, respectively. The three $[Mo_8\text{-ox}]^{2-}$, $[Mo_{10}\text{-glu}]^{2-}$, and $[Mo_{12}\text{-pim}]^{2-}$ molecular architectures consist of an

(8) (a) Coucouvanis, D.; Toupadakis, A.; Lane, J. D.; Koo, S. M.; Kim, C. G.; Hadjikyriakou, A. *J. Am. Chem. Soc.* **1991**, *113*, 5271. (b) Armstrong, F. A.; Shibahara, T.; Sykes, A. G. *Inorg. Chem.* **1978**, *1*, 189. (c) McDonald, W. S. *Acta Crystallogr.* **1978**, *B54*, 2850. (d) Kamenar, B.; Kaitner, B.; Strukan, N. *Croat. Chem. Acta* **1991**, *64* (3), 329. (e) Mennemann, K.; Mattes, R. *J. Chem. Res.* **1979**, *100*, 1343. (f) Simonnet-Jégat, C.; Toscano, R. A.; Robert, F.; Daran, J. C.; Sécheresse, F. *J. Chem. Soc., Dalton Trans.* **1994**, 1311.

(9) Cadot, E.; Salignac, B.; Halut, S.; Sécheresse, F. *Angew. Chem., Int. Ed. Engl.* **1998**, *37*, 611.

(10) Cadot, E.; Salignac, B.; Loiseau, T.; Dolbecq A.; Sécheresse F. *Chem. Eur. J.* **1999**, *5*, 3390.

(11) Cadot, E.; Salignac B.; Marrot, J.; Dolbecq A.; Sécheresse, F. *Chem. Commun.* **2000**, 261−262.

(12) Dolbecq, A.; Salignac, B.; Cadot E.; Sécheresse, F. *J. Chem. Soc., Chem. Commun.* **1998**, 2293.

Table 1. Summary of Crystal Structure Data

	$[NMe_4]_2[Mo_8\text{-ox}]\cdot 13H_2O$	$Cs_2[Mo_{10}\text{-glu}]\cdot 11H_2O$	$Rb_4glu[Mo_{10}\text{-glu}]\cdot 5H_2O$	$Cs_2[Mo_{12}\text{-pim}]\cdot 22H_2O$
formula	$C_{10}H_{44}N_2Mo_8O_{26}S_8$	$C_5H_{38}Cs_2Mo_{10}O_{35}S_{10}$	$C_{10}H_{32}Rb_4Mo_{10}O_{33}S_{10}$	$C_7H_{35}Cs_2Mo_{12}O_{50}S_{12}$
M, g mol^{-1}	1632.47	2204.17	2302.24	2721.17
T, K	296	293	296	293
crystal size, mm	0.40 × 0.40 × 0.36	0.30 × 0.20 × 0.12	0.18 × 0.06 × 0.04	0.30 × 0.20 × 0.12
crystal system	monoclinic	monoclinic	orthorhombic	monoclinic
space group	$P2_1/c$	$P2_1/c$	$Cmc2_1$	$C2/m$
a, Å	15.064(2)	13.5426(2)	24.296(4)	22.2850(1)
b, Å	13.013(3)	18.5523(2)	10.165(3)	11.0041(2)
c, Å	12.470(2)	22.5839(3)	21.828(6)	18.7617(3)
β, deg	112.73(1)	103.703(1)	90	123.007(1)
V, Å^3	2254.7(8)	5512.62(14)	5391(2)	3858.30(9)
Z	2	4	4	2
ρ_{calc}, g cm^{-3}	2.405	2.656	2.837	2.342
μ(Mo Kα), cm^{-1}	25.98	39.54	63.01	32.18
λ(Mo Kα), Å	0.71073	0.71073	0.71073	0.71073
θ range, deg	1.47−29.84	1.55−31.02	1.68−29.64	1.29−26.36
data collected	12 723	41 089	18 063	8732
unique data	5599	16 140	6440	2950
unique data $I > 2\sigma(I)$	4773	11 416	4233	2701
no. of parameters	228	527	289	222
$R(F)^a$	0.0309	0.0492	0.0600	0.0426
$R_w(F^2)^b$	0.0848	0.1299	0.1294	0.1187
GOF	1.057	0.995	1.114	1.086

^{a} $R_1 = \sum|F_o| - |F_c|/\sum|F_c|$. ^{b} $R_w = (\Sigma w(F_o^2 - F_c^2)^2/\sum w(F_o^2)^2)^{1/2}$; $1/w = \sigma^2F_o^2 + (aP)^2 + bP$.

inorganic cyclic neutral skeleton $\{Mo_{2n}S_{2n}O_{2n}(OH)_{2n}\}$, $n = 4$, 5, 6, respectively, encapsulating the guest linear dicarboxylate anion. The "wheel" results from $[Mo_2S_2O_2]^{2+}$ building blocks linked to each other by double hydroxo bridges. Two types of Mo−Mo distances are observed: short Mo−Mo distances (ca. 2.8 Å) within the dinuclear unit, characteristic of a metal−metal bond, and long Mo−Mo interblock distances (ca. 3.2 Å). Except for the nuclearity and the nature of the template, the most striking feature of these structures is the possibility for the Mo^V centers to occupy square pyramidal or octahedral sites. The combination of the two pyramidal and octahedral coordinations is at the origin of the great flexibility of these architectures. Indeed, the Mo−Mo−Mo angles can vary from 135° to 180°, while the interblock connections can be face-sharing or edge-sharing.

$[N(CH_3)_4]_2[Mo_8S_8O_8(OH)_8(C_2O_4)]\cdot 10H_2O$, $[NMe_4]_2[Mo_8\text{-ox}]\cdot 10H_2O$. The inorganic skeleton of the octameric ring (Figure 1a) results from the self-linking of four $\{Mo_2S_2O_2\}$ thiofragments. The eight Mo centers are octahedral with quite close Mo−Mo−Mo angles (about 135°). The connections between the dinuclear building blocks are exclusively face-shared. Each oxygen atom of the central oxalate group is doubly bonded to the two closest molybdenum atoms. Such an arrangement has been already observed in a fully oxygenated ring in which the $\{Mo_2O_4\}$ cores are bridged by methoxy groups.[13]

$Cs_2[Mo_{10}S_{10}O_{10}(OH)_{10}(H_6C_5O_4)]\cdot 11H_2O$, $Cs_2[Mo_{10}\text{-glu}]\cdot 11H_2O$. The labeled representation of the anion is shown Figure 1b. The presence of the central dicarboxylate lowers the symmetry of the cyclic skeleton, which appears strongly deformed in comparison with the pentagonal idealized D_{5h} symmetry of $[Mo_{10}S_{10}O_{10}(OH)_{10}(H_2O)_5]$.[11] The template-free and templated anions are shown in Figure 2. The unequivalent binding modes of the four oxygen atoms of the carboxylate groups reflect the lack of symmetry (Figure 2b). The oxygen atoms of the carboxylate group containing the C1 atom are singly bonded, the two related Mo−O distances (Mo6−O23 and Mo5−O24) being strictly equivalent [2.317(4) Å]. The coordination of the remaining carboxylate is quite different since the O22 oxygen atom is doubly bonded to Mo10 and Mo1 atoms, through bond lengths of 2.335(5) Å and 2.355(4) Å, while O21 is linked only to Mo9 [2.332(5) Å]. Mo1, Mo5, Mo6, Mo9, and Mo10 atoms are octahedral, while Mo2, Mo3, Mo4, Mo7, and Mo8 have a square pyramidal arrangement. No inner coordinated water was found trans to the Mo═O double bond, although the compound was synthesized and crystallized in water. Such a result is attributed to steric constraints induced by the presence of the bulky inner alkyl chain. Depending on the coordination of the Mo atoms, the nonbonding contacts between the building blocks are edge- or face-sharing. The three central carbons atoms, C2, C3, and C4, of the alkyl chain are disordered over two positions. Nevertheless, the two resulting conformations of the central alkyl chain, labeled A and B, are quite similar.

$Rb_4(H_6C_5O_4)[Mo_{10}S_{10}O_{10}(OH)_{10}(H_6C_5O_4)]\cdot 5H_2O$, $Rb_4glu[Mo_{10}\text{-glu}]\cdot 5H_2O$. The molecular arrangement of $[Mo_{10}S_{10}O_{10}(OH)_{10}(H_6C_5O_4)]^{2-}$ in $Rb_4glu[Mo_{10}\text{-glu}]\cdot 5H_2O$, represented in Figure 1c, is quite similar to that found in $Cs_2[Mo_{10}\text{-glu}]\cdot 5H_2O$. The coordination modes of the carboxylate groups are similar in both of the structures, the main difference lying in the disorder of the alkyl chain. A carboxylate group (C5, O13, O14) is delocalized over two equivalent positions generated by the mirror plane. In the solid state, the $[Mo_{10}S_{10}O_{10}(OH)_{10}(H_6C_5O_4)]^{2-}$ anions are connected through hydrogen bonds involving an outer glutarate anion and bridging hydroxo ligands of the ring (O6, O8). Short and long O−O distances corresponding to 2.63 and 2.85 Å alternately ensure the outer-glutarate/ring connections. Such an arrangement forms infinite zigzag chains, running along the c axis (Figure 3).

$Cs_2[Mo_{12}S_{12}O_{12}(OH)_{12}(H_{10}C_7O_4)]\cdot 20H_2O$, $Cs_2[Mo_{12}\text{-pim}]$. The overall molecular structure of the anion, depicted in Figure 1d, exhibits a 12-membered ring encapsulating the central pimelate anion. The Mo_{12} ring appears strongly distorted, the symmetry of the anion being lowered from idealized D_{6h} symmetry in the circular $[Mo_{12}S_{12}O_{12}(OH)_{12}(H_2O)_6]$[9] to C_{2h} in $[Mo_{12}\text{-pim}]^{2-}$ (Figure 4). The deformation due to the presence of the central dicarboxylate is comparable to that observed in the phosphate-containing Mo_{12} ring. In the $[(HPO_4)_2Mo_{12}S_{12}O_{12}(OH)_{12}(H_2O)_2]^{4-}$ anion,[10] the small size of the tetrahedral groups

(13) Chen, Q.; Liu, S.; Zubieta, J. *Angew. Chem., Int. Ed. Engl.* **1988**, *27*, 1724.

Table 2. Selected Bond Lengths (Å) for $[NMe_4]_2[Mo_8\text{-ox}]\cdot 13H_2O$ (a), $Cs_2[Mo_{10}\text{-glu}]\cdot 11H_2O$ (b), $Rb_4Glu[Mo_{10}\text{-glu}]\cdot 5H_2O$ (c), and $Cs_2[Mo_{12}\text{-pim}]\cdot 22H_2O$ (d)

(a) $[NMe_4]_2[Mo_8\text{-ox}]\cdot 13H_2O$

Mo(1)−O(1)	1.687(3)	Mo(3)−S(4)	2.3052(12)	Mo(4)−O(4)	1.684(3)
Mo(1)−O(8)	2.075(3)	Mo(3)−S(3)	2.3135(12)	Mo(4)−O(8)	2.076(3)
Mo(1)−O(7)	2.097(3)	Mo(3)−O(10)	2.479(3)	Mo(4)−O(7)	2.096(3)
Mo(1)−S(2)	2.3089(12)	Mo(3)−Mo(4)	2.8012(7)	Mo(4)−S(4)	2.3080(11)
Mo(1)−S(1)	2.3187(12)	Mo(2)−O(2)	1.679(3)	Mo(4)−S(3)	2.3160(12)
Mo(1)−O(9)	2.479(3)	Mo(2)−O(5)	2.080(3)	Mo(4)−O(9)	2.509(3)
Mo(1)−Mo(2)	2.8136(6)	Mo(2)−O(6)	2.106(3)	C(1)−C(2)	1.074(12)
Mo(3)−O(3)	1.685(3)	Mo(2)−S(2)	2.3072(12)	C(1)−C(2)	1.100(12)
Mo(3)−O(5)	2.078(3)	Mo(2)−S(1)	2.3125(12)	C(1)−O(9)	1.292(6)
Mo(3)−O(6)	2.101(3)	Mo(2)−O(10)	2.470(3)	C(1)−C(1)	1.544(11)

(b) $Cs_2[Mo_{10}\text{-glu}]\cdot 11H_2O$

Mo(1)−O(1)	1.675(4)	Mo(5)−O(16)	2.109(4)	Mo(9)−O(19)	2.106(4)
Mo(1)−O(11)	2.088(4)	Mo(5)−O(24)	2.291(4)	Mo(9)−S(9)	2.316(2)
Mo(1)−O(12)	2.120(4)	Mo(5)−S(5)	2.314(2)	Mo(9)−S(10)	2.325(2)
Mo(1)−S(1)	2.309(2)	Mo(5)−S(6)	2.320(2)	Mo(9)−O(21)	2.332(5)
Mo(1)−S(2)	2.315(2)	Mo(5)−Mo(6)	2.8187(7)	Mo(9)−Mo(10)	2.8314(7)
Mo(1)−O(22)	2.355(4)	Mo(6)−O(6)	1.684(4)	Mo(10)−O(10)	1.685(4)
Mo(1)−Mo(2)	2.8394(7)	Mo(6)−O(17)	2.089(4)	Mo(10)−O(11)	2.103(4)
Mo(2)−O(2)	1.681(4)	Mo(6)−O(18)	2.108(4)	Mo(10)−O(12)	2.121(4)
Mo(2)−O(14)	2.067(4)	Mo(6)−O(23)	2.317(4)	Mo(10)−S(10)	2.315(2)
Mo(2)−O(13)	2.080(4)	Mo(6)−S(6)	2.318(2)	Mo(10)−S(9)	2.319(2)
Mo(2)−S(2)	2.310(2)	Mo(6)−S(5)	2.325(2)	Mo(10)−O(22)	2.335(5)
Mo(2)−S(1)	2.315(2)	Mo(7)−O(7)	1.674(5)	C(1)−O(23)	1.288(8)
Mo(3)−O(3)	1.672(4)	Mo(7)−O(17)	2.090(4)	C(1)−O(24)	1.245(9)
Mo(3)−O(13)	2.061(4)	Mo(7)−O(18)	2.090(4)	C(1)−C(2B)	1.52(2)
Mo(3)−O(14)	2.062(4)	Mo(7)−S(8)	2.320(2)	C(2B)-C(3B)	1.52(2)
Mo(3)−S(4)	2.309(2)	Mo(7)−S(7)	2.321(2)	C(3B)-C(4B)	1.56(2)
Mo(3)−S(3)	2.310(2)	Mo(7)−O(23)	2.517(5)	C(4B)-C(5)	1.54(2)
Mo(3)−Mo(4)	2.8404(7)	Mo(7)−Mo(8)	2.8239(7)	C(1)−C(2A)	1.55(2)
Mo(4)−O(4)	1.675(4)	Mo(8)−O(8)	1.686(4)	C(2A)-C(3A)	1.56(2)
Mo(4)−O(16)	2.061(4)	Mo(8)−O(20)	2.049(4)	C(3A)-C(4A)	1.61(2)
Mo(4)−O(15)	2.063(4)	Mo(8)−O(19)	2.072(4)	C(4A)-C(5)	1.58(2)
Mo(4)−S(3)	2.314(2)	Mo(8)−S(8)	2.308(2)	C(5)−O(22)	1.233(10)
Mo(4)−S(4)	2.319(2)	Mo(8)−S(7)	2.308(2)	C(5)−O(21)	1.276(10)
Mo(5)−O(5)	1.705(5)	Mo(9)−O(9)	1.680(4)		
Mo(5)−O(15)	2.087(4)	Mo(9)−O(20)	2.083(4)		

(c) $Rb_4Glu[Mo_{10}\text{-glu}]\cdot 5H_2O$

Mo(1)−O(1)	1.672(11)	Mo(2)−Mo(3)	2.844(2)	Mo(4)−Mo(5)	2.847(2)
Mo(1)−O(6)	2.076(10)	Mo(3)−O(3)	1.652(11)	Mo(5)−O(5)	1.686(11)
Mo(1)−O(7)	2.129(10)	Mo(3)−O(9)	2.046(10)	Mo(5)−O(10)	2.101(9)
Mo(1)−O(12)	2.264(11)	Mo(3)−O(8)	2.081(11)	Mo(5)−O(11)	2.132(8)
Mo(1)−S(2)	2.314(5)	Mo(3)−S(4)	2.315(4)	Mo(5)−S(6)	2.317(4)
Mo(1)−S(1)	2.334(5)	Mo(3)−S(3)	2.317(4)	Mo(5)−S(5)	2.313(4)
Mo(1)−Mo(1)	2.817(3)	Mo(4)−O(4)	1.679(10)	Mo(5)−O(14)	2.364(10)
Mo(2)−O(2)	1.639(11)	Mo(4)−O(9)	2.048(11)	C(1)−O(12)	1.28(2)
Mo(2)−O(6)	2.075(10)	Mo(4)−O(8)	2.092(10)	C(1)−C(2)	1.47(4)
Mo(2)−O(7)	2.089(9)	Mo(4)−O(13)	2.35(2)	C(2)−C(3)	1.49(3)
Mo(2)−S(4)	2.304(4)	Mo(4)−S(5)	2.311(4)	C(3)−C(4)	1.41(7)
Mo(2)−S(3)	2.313(4)	Mo(4)−S(6)	2.334(4)	C(4)−C(5)	1.31(7)

(d) $Cs_2[Mo_{12}\text{-pim}]\cdot 22H_2O$

Mo(1)−O(1)	1.684(10)	Mo(3)−O(10)	2.341(12)	Mo(5)−Mo(6)	2.807(2)
Mo(1)−O(9)	2.051(7)	Mo(3)−Mo(4)	2.810(2)	Mo(6)−O(6)	1.666(10)
Mo(1)−S(1)	2.294(3)	Mo(4)−O(4)	1.691(10)	Mo(6)−O(9)	2.053(7)
Mo(1)−Mo(2)	2.799(2)	Mo(4)−O(8)	2.091(7)	Mo(6)−S(3)	2.297(3)
Mo(2)−O(2)	1.659(11)	Mo(4)−S(2)	2.309(3)	C(1)−O(10)	1.27(2)
Mo(2)−O(7)	2.043(7)	Mo(4)−O(11)	2.359(9)	C(1)−O(11)	1.27(2)
Mo(2)−S(1)	2.306(3)	Mo(5)−O(5)	1.678(10)	C(1)−C(2)	1.47(3)
Mo(3)−O(3)	1.666(11)	Mo(5)−O(8)	2.085(6)	C(2)−C(3)	1.51(5)
Mo(3)−O(7)	2.096(8)	Mo(5)−S(3)	2.312(3)	C(3)−C(4)	1.50(7)
Mo(3)−S(2)	2.318(3)	Mo(5)−O(11)	2.440(9)	C(3)−C(4)	1.50(7)

makes possible the coordination of two water molecules in the cavity. Conversely, in $[Mo_{12}S_{12}O_{12}(OH)_{12}(C_7H_{10}O_4)]^{2-}$, the bulky inner alkyl chain prevents any coordination of water molecules.

Synthesis. At pH 4−5, addition of the various organic acids to a solution of $\{K_{0.40}(NMe_4)_{0.1}I_{0.5}[Mo_2S_2O_2(OH)_2(H_2O)]\cdot 6.3H_2O\}_n$ directly leads to the formation of templated rings. The condensation products were characterized in solution by NMR and ESMS techniques (see below). In the presence of oxalate, glutarate, or pimelate, the Mo_8, Mo_{10}, and Mo_{12} rings are the major species present in solution, demonstrating that the $\{Mo_{2n}S_{2n}O_{2n}(OH)_{2n}\}$ cyclic backbone is flexible and versatile enough to rearrange itself in the appropriate size and shape imposed by the dicarboxylate anion. Thus, for such systems, the nuclearity of the species is dictated by the nature of the template. We previously reported a study illustrating the competition between the chelating and templating roles of the oxalate anions.[14] About pH 1, oxalate ions have only a chelating

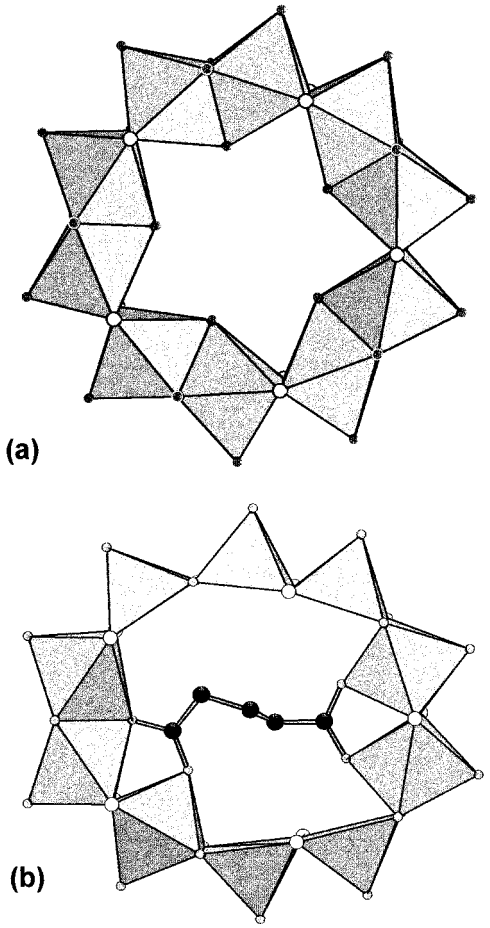

Figure 2. Polyhedral views illustrating the deformation of the Mo_{10} ring upon coordination of the central carboxylate, from D_{5h} idealized symmetry in $[Mo_{10}S_{10}O_{10}(OH)_{10}(H_2O)_5]$ (a) to the templated Mo_{10} ring (b).

behavior. Between pH 2 and 4, the two effects are observed, since the resulting compound consists of two oxalato dinuclear units bridged by a central oxalate, initiating the template influence. Above pH 4, the self-condensation process prevails over the chelating properties of oxalate, leading to the templated Mo_8 ring. $[Mo_8S_8O_8(OH)_8(C_2O_4)]^{2-}$ ($[Mo_8\text{-ox}]^{2-}$), $[Mo_{10}S_{10}O_{10}(OH)_{10}(C_5H_6O_4)]^{2-}$ ($[Mo_{10}\text{-glu}]^{2-}$), and $[Mo_{12}S_{12}O_{12}(OH)_{12}(C_7H_{10}O_4)]^{2-}$ ($[Mo_{12}\text{-pim}]^{2-}$) were quantitatively isolated in the solid state by precipitation or crystallization. For $[Mo_{10}\text{-glu}]^{2-}$, the initial stoiechiometry [glutarate]/$\{Mo_2S_2O_2\}$ has no effect on the nature of the isolated molecular backbone since the Mo_{10} ring containing a glutarate template is systematically obtained. Therefore, with excess of glutarate, the formed $Rb_4glu[Mo_{10}\text{-glu}]\cdot 5H_2O$ displays a supramolecular arrangement involving an additional outer glutarate anion (Figure 3).

Distribution in Solution. Electrospray mass spectrometry (ESMS) has been performed at pH 4.5 on $MeOH-H_2O$ solutions containing mixtures of dilute $[Mo_2S_2O_2]^{2+}$ (about 8×10^{-2} mol L^{-1}) and carboxylate. ESMS spectra of the ox^{2-}, glu^{2-}, and pim^{2-} systems are shown in Figure 5, and spectroscopic data are given in Table 3. In the ESMS spectrum of each sample, the parent peak of the expected molecular anion is clearly observed and represents the predominant species in solution. The experimental m/z values correspond exactly to those deduced from the single-crystal X-ray data. The patterns of the oxalato sample exhibit an intense peak (92%) at $m/z =$ 686 which was unambiguously attributed to the octameric $[Mo_8S_8O_8(OH)_8(C_2O_4)]^{2-}$. Similarly, ESMS spectra of glu^{2-} and

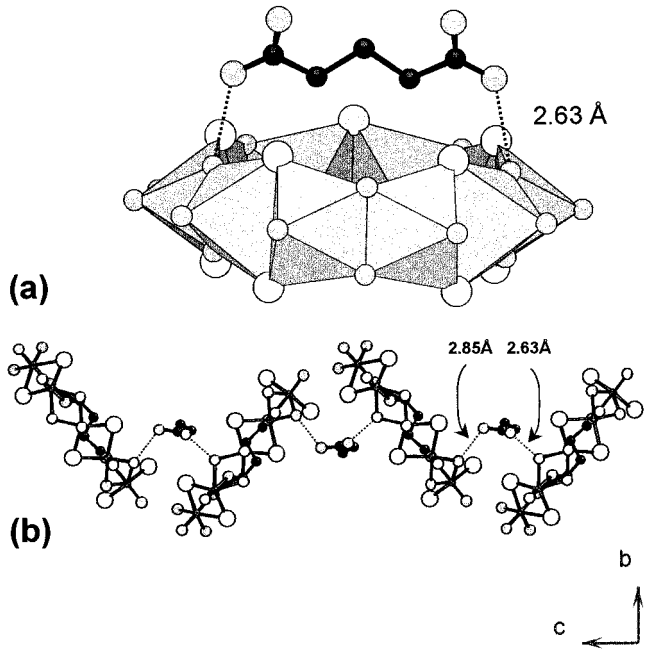

Figure 3. Hydrogen-bonding pattern in the solid state between carboxylate groups of an additional outer glu^{2-} and hydroxo bridges of the $[Mo_{10}\text{-glu}]^{2-}$ in $Rb_4glu[Mo_{10}\text{-glu}]\cdot 5H_2O$ (a). Zigzag chain resulting from the alternance of short (2.63 Å) and long O−O (2.85 Å) distances (b).

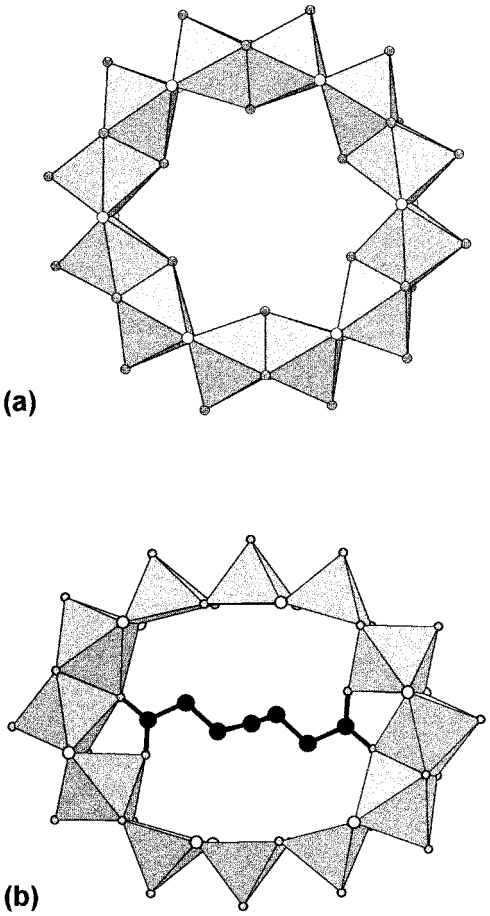

Figure 4. Polyhedral views showing the lowering of the symmetry from D_{6h} in the $[Mo_{12}S_{12}O_{12}(OH)_{12}(H_2O)_6]$ neutral complex (a) to C_2 in the templated $[Mo_{12}\text{-pim}]^{2-}$ anion (b).

(14) Dolbecq, A.; Salignac, B.; Cadot, E.; Sécheresse, F. *Bull. Pol. Acad. Sci.* **1998**, *46*, 237.

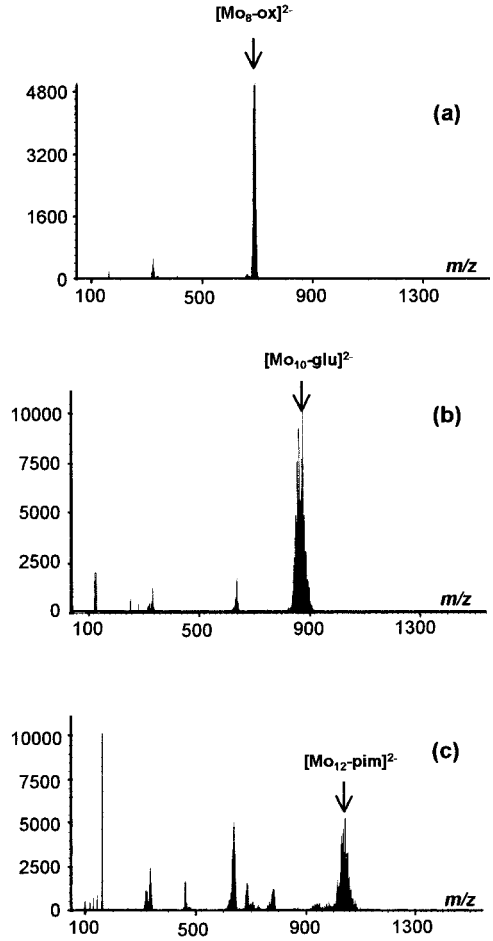

Figure 5. ESMS spectra of a mixture of dilute $[Mo_2S_2O_2]^{2+}$ solutions at pH 4.5 with oxalate (a), glutarate (b), and pimelate ions (c).

Table 3. Negative-Ion ESMS Data of $[Mo_2S_2O_2]^{2+}$/Dicarboxylates Systems at pH 4.5

samples	*m/z*, exptl (*I*, %)	empirical formula	*m/z*, theor
ox^{2-}	686 (92)	$[Mo_8S_8O_8(OH)_8(C_2O_4)]^{2-}$	688
	664 (2)		
	321 (6)		
glu^{2-}	868 (93)	$[Mo_{10}S_{10}O_{10}(OH)_{10}(H_6C_5O_4)]^{2-}$	870
	638 (4)		
	334 (2)		
	321 (1)		
pim^{2-}	1043 (52)	$[Mo_{12}S_{12}O_{12}(OH)_{12}(H_{10}C_7O_4)]^{2-}$	1045
	785 (5)		
	685 (7)		
	638 (26)		
	461 (2)		
	334 (5)		
	321 (3)		

pim^{2-} solutions reveal the presence of the decameric $[Mo_{10}S_{10}O_{10}(OH)_{10}(H_6C_5O_4)]^{2-}$ ($m/z = 870$) and the dodecameric $[Mo_{12}S_{12}O_{12}(OH)_{12}(H_{10}C_7O_4)]^{2-}$ anions ($m/z = 1043$). Other species were detected in solution together with the previously identified polymeric rings. A peak of $m/z = 321$ is observed in all the spectra, while the $m/z = 638$ peak is common only to glu^{2-} and pim^{2-} spectra. These different peaks were attributed to template-free anionic species such as $[H_3Mo_4S_4O_8]^-$ ($m/z = 643$) and $[H_2Mo_4S_4O_8]^{2-}$ ($m/z = 321$), which probably have linear enchainments. Other possibilities could be postulated, but definitive attributions would need other ESMS investigations. The evidence and the proportion of those species are probably related to the ESMS technique since the desolvation of the anions by the drying agent may interfere in the equilibrium process, revealing a distribution in the spray different from that of the bulk solution. Such a behavior has already been observed by Howarth and co-workers, who reported that the distribution of polyoxometalates, such as tungstates or molybdates, was extremely sensitive to ESMS conditions.[15]

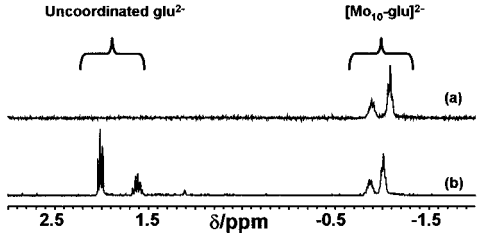

Figure 6. ^1H NMR spectra of $Cs_2[Mo_{10}\text{-glu}]\cdot 11H_2O$ (a) and $Rb_4glu[Mo_{10}\text{-glu}]\cdot 5H_2O$ (b) in D_2O.

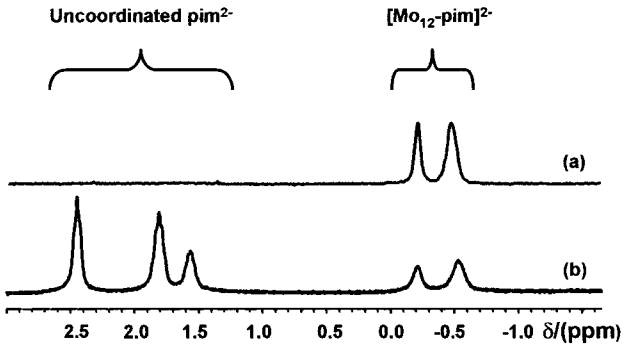

Figure 7. ^1H NMR spectra of pure $Cs_2[Mo_{12}\text{-pim}]\cdot 22H_2O$ (a) and a synthetic mixture of $Cs_2[Mo_{12}\text{-pim}]\cdot 22H_2O$ and H_2pim (b), in D_2O.

Dynamics. The fluxionality and molecular dynamics of the rings were studied by ^1H NMR experiments, in deuterium oxide and in acetonitrile-d_3, at variable temperature.

^1H NMR in D_2O. ^1H NMR spectra of pure $Cs_2[Mo_{10}S_{10}O_{10}(OH)_{10}(H_6C_5O_4)]\cdot 11H_2O$ and $Rb_4(H_6C_5O_4)[Mo_{10}S_{10}O_{10}(OH)_{10}(H_6C_5O_4)]\cdot 5H_2O$ are shown in Figure 6a. The spectrum of $Cs_2[Mo_{10}\text{-glu}]\cdot 11H_2O$ exhibits a quintuplet at -0.86 ppm and a triplet at -1.01 ppm with a 1:2 intensity ratio attributed to the CH_2 groups of the encapsulated glutarate. The spectrum of $Rb_4glu[Mo_{10}\text{-glu}]\cdot 11H_2O$, shown in Figure 6a, contains additional resonances attributed to the presence of an uncoordinated glutarate anion per ring, in agreement with the results of the solid-state structure. The spectrum of $[Mo_{12}\text{-pim}]^{2-}$, given in Figure 7a, exhibits two broad lines at -0.20 and -0.53 ppm corresponding to the resonances of the CH_2 groups of the encapsulated pimelate. On the basis of its intensity, the -0.20 ppm line was attributed to one group of two equivalent CH_2's, while the -0.53 ppm peak was assigned to the overlapped resonances of the two remaining equivalent CH_2 groups with those of the central CH_2 group. The spectrum of a synthetic mixture containing pure $[Mo_{12}\text{-pim}]^{2-}$ ring and uncoordinated pimelate exhibits three additional resonances, at 2.44, 1.80, and 1.56 ppm, of 2:2:1 relative intensity, as expected for the 10 protons of the uncoordinated pimelate (Figure 7b). The screening of the CH_2 groups of the encapsulated alkyl chain represents a good probe to characterize in solution the templated inorganic ring. No other species was observed in solution, in equilibrium with $[Mo_{10}\text{-glu}]^{2-}$ or $[Mo_{12}\text{-pim}]^{2-}$, confirming the chelating behavior of the inner dicarboxylates which prevents any exchange reaction.

Variable Temperature in CD_3CN. The variable-temperature ^1H NMR spectra of $Li_2[Mo_{10}\text{-glu}]\cdot 11H_2O$, $Li_2[Mo_{12}\text{-pim}]\cdot$

(15) Deery, M. J.; Howarth, O. J.; Jennings, K. R. *J. Chem. Soc., Dalton Trans.* **1996**, 2629.

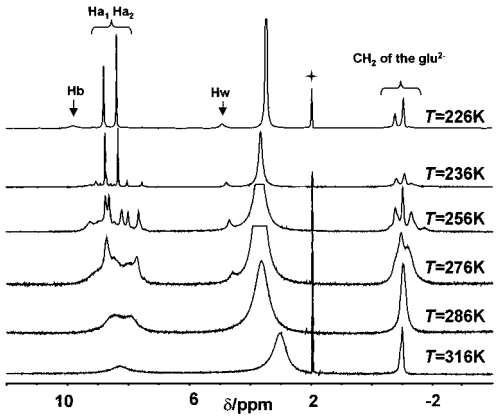

Figure 8. Variable-temperature ^{1}H NMR spectra of $Li_2[Mo_{10}\text{-glu}]\cdot 11H_2O$ in CD_3CN (+: solvent impurity).

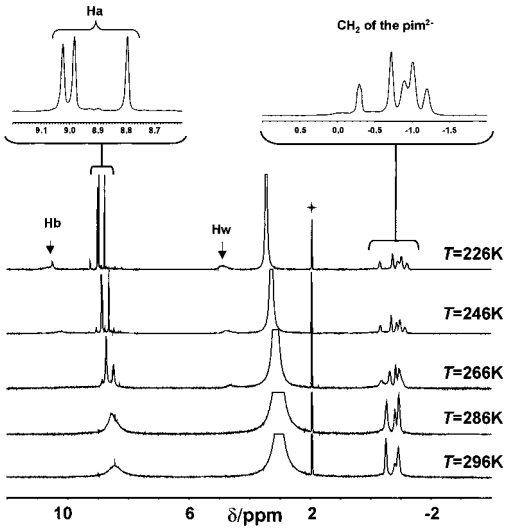

Figure 9. Variable-temperature ^{1}H NMR spectra of $Li_2[Mo_{12}\text{-pim}]\cdot 22H_2O$ in CD_3CN (+: solvent impurity) at 236 and 346 K.

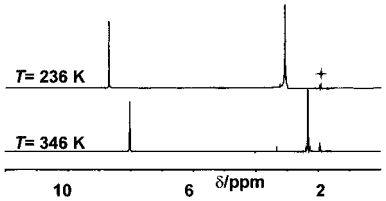

Figure 10. Variable-temperature ^{1}H NMR spectra of $Li_2[Mo_8\text{-ox}]\cdot 18.5H_2O$ in CD_3CN (+: solvant impurity).

$22H_2O$, and $Li_2[Mo_8\text{-ox}]\cdot 18.5H_2O$ in CD_3CN are represented in Figures 8, 9, and 10, respectively, and selected ^{1}H NMR data are reported in Table 4.

$Li_2[Mo_{10}\text{-glu}]\cdot 11H_2O$. In Figure 8 are given the ^{1}H NMR spectra of $Li_2[Mo_{10}\text{-glu}]\cdot 11H_2O$. They contain three groups of signals, as expected for the three types of protons present in the alkyl chain, water, and hydroxo bridges. The peaks related to the CH_2 groups of the central dicarboxylate are observed between 0.0 and −1.0 ppm with chemical shifts close to those determined in D_2O. The water signals are located in the 4−2 ppm range, while the most deshielded resonances within the 7−10 ppm region are attributed to protons of the double hydroxo bridges, ensuring the interblock connections. Such chemical shifts have been previously observed for protons attached to polymetalates. A. G. Wedd et al., in a complete multinuclear NMR study (^{1}H and ^{183}W) on the six-electron-reduced metatungstate anion α-$[H_2[W^{IV}(H_2O)]_3W^{VI}{}_9O_{34}(OH)_3]^{3-}$,[16] reported

Table 4. Summary of the ^{1}H NMR Data of $Li_2[Mo_8\text{-ox}]$, $Li_2[Mo_{10}\text{-glu}]$, and $Li_2[Mo_{12}\text{-pim}]$ in CD_3CN

		chemical shifts (relative intensity)	
compound	*T*, K	inorganic protons	organic protons
$[Mo_8\text{-ox}]^{2-}$	346	8.02	
	236	8.82	
$[Mo_{10}\text{-glu}]^{2-}$	316	8.25 (5)	−1.11 (1)
			−0.98 (2)
	226	9.78 (1)	−0.78 (1)
		8.78 (2)	−1.06 (2)
		8.36 (2)	
		4.91 (2)	
$[Mo_{12}\text{-pim}]^{2-}$	316	8.45 (6)	−0.49 (2)
			−0.79 (1)
			−0.90 (2)
	226	10.63 (2)	−0.29 (1)
		10.50 (1)	−0.72 (2)
		9.02 (2)	−0.89 (1)
		8.92 (2)	−0.98 ($^1/_2$)
		8.79 (2)	−1.01 (2)
			−1.19 (1)
		4.98 (0.8)	
		4.84 (3.2)	

that the resonances of the 11 protons present in the polyanion of C_s symmetry are located in the 7.0−9.0 ppm region.

The signals of the protons of the alkyl chain and of the inorganic hydroxo bridges have an intensity ratio of 0.6, which exactly corresponds to the six protons of the three CH_2 groups and the 10 protons of the 10 hydroxo bridges. While the temperature is decreased, the ^{1}H NMR spectrum of $[Mo_{10}\text{-glu}]^{2-}$ undergoes drastic changes, simultaneously observed on the regions corresponding both to the bridge resonances and to the CH_2 groups of the dicarboxylate. The broad peak observed at 316 K, attributed to the hydroxo bridges, gradually splits into several sharp lines, to display 10 resonances at 256 K. Simultaneously, seven identified lines arise from the two 1:2 overlapped lines of the central glutarate, initially observed at 316 K. Below 256 K, the complexity of the ^{1}H pattern decreases simultaneously in both the regions. At 226 K, the resonances of hydroxo bridges and glutarate consist only of five main peaks at 9.78, 8.78, and 8.36 ppm and −0.78 and −1.06 ppm, respectively. The intensities of these lines (1:2:2 and 1:2, respectively) agree with a postulated C_{2v} symmetry for the anion. Such a symmetry is higher than that determined in the crystal by X-ray diffraction and corresponds to a symmetric conformation of the central alkyl chain. Below 276 K, an additional line separates from that of uncoordinated water (between 3 and 4 ppm) and gradually shifts to reach 4.91 ppm at 226 K. This additional peak was related to water exchange because the square pyramidal molybdenum atoms can bind a single water molecule. The presence of one aquo ligand (2Hw) is in agreement with the relative intensity of the 4.91 ppm line. A possible polyhedral representation of the C_{2v} conformer is given in Figure 11. On the basis of its intensity, the broad signal at 9.80 ppm is assigned to the two equivalent protons labeled Hb, while the two remaining sharp lines at 8.80 and 8.40 ppm are attributed to the four equivalent Ha_1 and Ha_2 protons.

The different changes observed in the ^{1}H NMR spectra of $[Mo_{10}\text{-glu}]^{2-}$ (Figure 8) are directly related to the fluxionality of the molecule. At room temperature, the central glutarate guest randomly wheels in the cavity, owing to the concerted hopping of the two terminal carboxylate groups over the 10 molybdenum atoms. Such a dynamic is strongly supported by the versatility

(16) Boskovic, C.; Sadek, M.; Brownlee, R. T. C.; Bond, A.; Wedd, A. G. *Chem. Commun.* **1999**, 533−534.

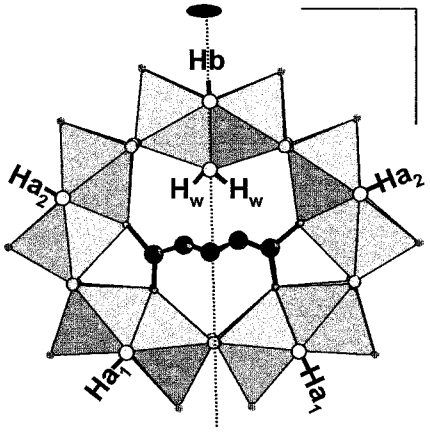

Figure 11. Postulated frozen arrangement at 226 K of the central glu^{2-} in the Mo_{10} ring. The ring of C_{2v} symmetry displays four groups of equivalent protons (4 Ha_1, 4 Ha_2, 2Hb, 2Hw).

of the Mo^V atoms, which can adopt octahedral and pyramidal coordination. The internal rotation of the dicarboxylate and the exchange of aquo ligands both decrease with temperature. At 226 K, the hopping of the dicarboxylate is totally hampered on the NMR time scale, which gives a single frozen C_{2v} conformation containing a water molecule (2Hw) coordinated to a Mo atom (Figure 11).

$Li_2[Mo_{12}$-pim]·22H_2O. The behavior of $[Mo_{12}\text{-pim}]^{2-}$ is quite similar to that of $[Mo_{10}\text{-glu}]^{2-}$ (see Figure 9). The averaged shape of the hydroxo resonances at 8.35 ppm together with the number and relative intensities of the CH_2 groups (2:1:2 at −0.49, −0.79, and −0.90 ppm, respectively) suggest a rapid internal motion of the central organic part. As the temperature is decreased, the single hydroxo broad line splits into several resonances while five lines are observed for the alkyl chain. The deconvolution of the CH_2 resonances at 226 K agrees with two sets of 2:1:2 lines at −0.29, −0.98, −1.19 ppm and −0.72, −0.89, −1.01 ppm, respectively. This result probably corresponds to the presence of two distinct conformations of the C_7 chain, in a 1:2 proportion, in agreement with the relative intensities of the two signals. At 226 K, the hydroxo bridges are characterized by five main lines at 10.63, 10.50, 9.02, 8.92, and 8.79 ppm of 2:1:2:2:2 relative intensities, corresponding to 12 protons present in the two cyclic conformers. A first set of three lines of 2:2:2 intensities corresponds to 12 protons (4Hb, 4Ha_1, 4Ha_2) distributed in a wheel of C_{2v} symmetry represented in Figure 12a. The remaining two lines of relative 1:2 intensities are attributed to a D_{2h} conformer which corresponds to the more symmetrical distribution (4Hb, 8Ha) represented in Figure 12b. According to the two sets of lines, the C_{2v} and D_{2h} conformers are in the 2:1 proportion. Thus, the three sharp lines at 9.02, 8.92, and 8.79 ppm, represented in the expanded part of Figure 9, could be attributed to the Ha protons, while the broad resonances at 10.63 and 10.50 ppm would correspond to the Hb protons. At 266 K, two overlapped lines, attributed to coordinated water, begin to separate from the broad signal of uncoordinated water to reach the 4.98 and 4.84 ppm values at 226 K. Such a feature has been previously observed in the ^1H NMR spectra of $[Mo_{10}\text{-glu}]^{2-}$ and corresponds to the decrease of the water exchange rate as the internal motion of the C_7 chain is hampered. Both of the signals could be related to the presence of coordinated water in the C_{2v} and D_{2h} conformers.

$Li_2[Mo_8$-ox]·18.5H_2O. At 346 K, the ^1H NMR spectrum of $[Mo_8\text{-ox}]^{2-}$ in CD_3CN (Figure 10) contains two sharp lines at 2.31 and 8.02 ppm, attributed to uncoordinated water and to the eight equivalent hydroxo bridges, but does not exhibit any significant temperature dependence. Such a behavior means that the rigidity of the octanuclear backbone is strongly ensured by the central oxalate. In such an arrangement, all of the Mo atoms are octahedral, which forbids any concerted internal rotation of the central caboxylate. Furthermore, in agreement with these features, no inner water exchange was obviously evidenced.

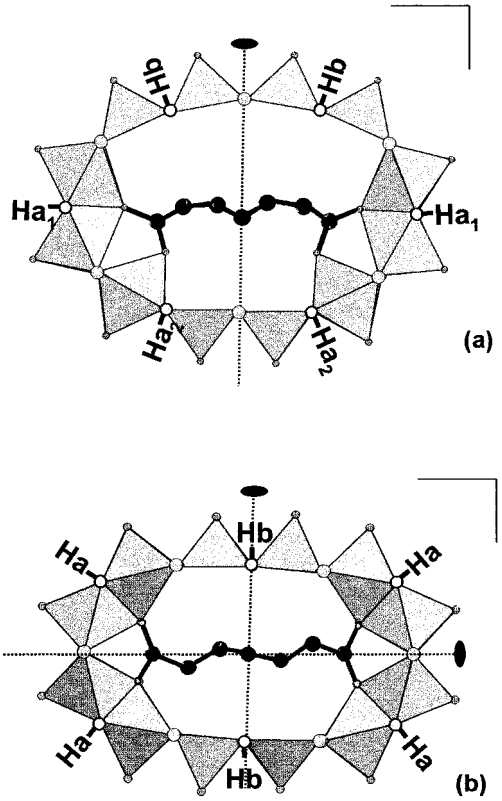

Figure 12. Postulated frozen arrangements of the two conformers $[Mo_{12}\text{-pim}]^{2-}$ in equilibrium at 226 K: the C_{2v} conformer (a) and the D_{2h} conformer (b) are in a 1:2 ratio in solution.

Experimental Section

Synthesis of $[N(CH_3)_4]_2[Mo_8S_8O_8(OH)_8(C_2O_4)]$·13$H_2O$, $[NMe_4]_2$-$[Mo_8$-ox]·13H_2O. The crude precursor $\{K_{0.4}(N(CH_3)_4)_{0.1}I_{0.5}[Mo_2S_2O_2$-$(OH)_2(H_2O)]\cdot 6.3H_2O\}_n$ (1.07 g, 2.0/*n* mmol) was hydrolyzed in 10 mL of a 4 mol L^{-1} aqueous solution of hydrochloric acid under vigorous stirring and mild heating (50 °C). Oxalic acid (0.30 g, 2.4 mmol) was added to the red-orange solution of the thiocation, and the pH of the solution was adjusted to 5 by slow addition of a 4 mol L^{-1} sodium hydroxide solution. The resulting red solution was filtered and allowed to stand at room temperature for crystallization. After a week, red cubic crystals of $[NMe_4]_2[Mo_8\text{-ox}]\cdot 13H_2O$ suitable for the X-ray structure determination were collected. Anal. Calcd (found): N, 1.59 (1.62); C, 6.82 (7.18); S, 14.56 (14.61); Mo, 43.68 (43.46).

Synthesis of $Cs_2[Mo_{10}S_{10}O_{10}(OH)_{10}(H_6C_5O_4)]$·11$H_2O$, $Cs_2[Mo_{10}$-glu]·11H_2O. The crude solid $\{K_{0.4}(N(CH_3)_4)_{0.1}I_{0.5}[Mo_2S_2O_2(OH)_2$-$(H_2O)]\cdot 6.3H_2O\}_n$ (1.07 g, 2.0/*n* mmol) was dissolved in 20 mL of water under vigorous stirring and mild heating (50 °C). $Na_2H_6C_5O_4$ (0.08 g; 0.45 mmol) was added to the solution, provoking a rapid color change from yellow to red (pH 5.5). Addition of cesium chloride (1.0 g, 5.9 mmol) precipitated an orange-red solid which was isolated by filtration and dried in air. The product was dissolved in 130 mL of water under mild agitation, and after 30 min, cesium chloride (3.0 g, 17.8 mmol) was added to the solution. The resulting solid $Cs_2[Mo_{10}\text{-glu}]$ was isolated by filtration and dried in air (yield 0.80 g, 94% based on Mo). Cs_2-$[Mo_{10}$-glu] was obtained as single crystals suitable for X-ray diffraction studies by recrystallization: 0.20 g of $Cs_2[Mo_{10}\text{-glu}]$ was dissolved in 20 mL of water. The solution was filtered and the filtrate covered for 2 weeks at room temperature to give yellow-orange crystals. Anal. Calcd

(found): C, 2.72 (2.61); Mo, 43.55 (43.11); S, 14.52 (13.93); Cs, 12.06 (13.20). IR spectra (KBr pellets, ν/cm^{-1}): 1564w, 1531m, 1459w, 1418w, 1311w, 1265w, 1105w, 960s, 942sh., 678w, 512s, 415w, 351m.

Synthesis of $Rb_4(H_6C_5O_4)[Mo_{10}S_{10}O_{10}(OH)_{10}(H_6C_5O_4)]\cdot 5H_2O$, $Rb_4glu[Mo_{10}\text{-}glu]\cdot 5H_2O$. The crude product $\{K_{0.4}(N(CH_3)_4)_{0.1}I_{0.5}[Mo_2S_2O_2(OH)_2(H_2O)]\cdot 6.3H_2O\}_n$ (1.07 g, 2/*n* mmol) was dissolved in 35 mL of water under vigorous stirring and mild heating (50 °C). $Na_2H_6C_5O_4$ (0.24 g, 1.35 mmol) was added (pH 6). RbCl (2.0 g, 16.5 mmol) was added and the mixture filtered. The resulting red solution was allowed to stand at room temperature for crystallization. After 4 days, red crystals of $Rb_4glu[Mo_{10}\text{-}glu]\cdot 5H_2O$ suitable for X-ray structure determination were collected. Anal. Calcd (found): C, 5.21 (5.08); Mo, 41.70 (40.92); S, 13.90 (13.79); Rb, 14.85 (13.90).

Synthesis of $Cs_2[Mo_{12}S_{12}O_{12}(OH)_{12}(C_7H_{10}O_4)]\cdot 22H_2O$, $Cs_2[Mo_{12}\text{-}pim]\cdot 22H_2O$. The crude compound $\{K_{0.4}(N(CH_3)_4)_{0.1}I_{0.5}[Mo_2O_2S_2(OH)_2(H_2O)]\cdot 6.3H_2O\}_n$ (1.07 g, 2.0/*n* mmol) was hydrolyzed in 5 mL of a 4 mol L^{-1} aqueous solution of hydrochloric acid under vigorous stirring. Pimelic acid (0.30 g, 1.9 mmol) was added to the red solution and the pH adjusted to 5.5 by slow addition of a 4 mol L^{-1} hydroxide potassium solution. The precipitate formed was isolated by suction, washed with ethanol, and dried with ether. The pale yellow solid was redissolved in 30 mL of water under vigorous stirring and moderate heating (50 °C), and the turbid solution was filtered. $Cs_2[Mo_{12}\text{-pim}]$ (0.60 g, 69% based on Mo) was isolated as a yellow-orange solid by addition of cesium chloride (1.50 g, 8.9 mmol). $Cs_2[Mo_{12}\text{-pim}]$ was obtained as single crystals suitable for X-ray diffraction studies by recrystallization: 0.20 g of $Cs_2[Mo_{12}\text{-pim}]$ was dissolved in 30 mL of water. The solution was filtered and the filtrate covered for 2 weeks at room temperature to yield yellow-orange crystals. Anal. Calcd (found): C, 3.05 (2.55); Mo, 41.86 (38.72); S, 13.95 (13.30); Cs, 9.66 (11.8). IR spectra (KBr pellets, ν/cm^{-1}): 1513m, 1467w, 1455w, 1413w, 1283w, 1227w, 1105w, 968s, 950s, 933s, 899w, 789w, 659w, 512s, 421w, 335m.

Synthesis of $Li_2[Mo_8S_8O_8(OH)_8(C_2O_4)]\cdot 18.5\ H_2O$, $Li_2[Mo_8\text{-ox}]\cdot 18.5H_2O$. The procedure is similar to that used for $[NMe_4]_2[Mo_8\text{-ox}]$ except the pH of the solution was adjusted to 5 by dropwise addition of a solution of 4 mol L^{-1} LiOH. The solution was carefully filtered and the filtrate allowed to stand at room temperature for crystallization. After a week, orange parallelepipedic well-shaped crystals of $Li_2[Mo_8\text{-ox}]\cdot 18.5H_2O$ were collected. Anal. Calcd (found): Li, 0.80 (0.73); C, 1.39 (1.48); S, 14.86 (14.84); Mo, 44.59 (44.51).

Preparation of $Li_2[Mo_{10}\text{-}glu]\cdot 11H_2O$ and $Li_2[Mo_{12}\text{-pim}]\cdot 22H_2O$. The two lithium salts were obtained from the corresponding cesium pure salts $Cs_2[Mo_{10}\text{-}glu]\cdot 11H_2O$ and $Cs_2[Mo_{12}\text{-pim}]\cdot 22H_2O$ previously dissolved in water. Each solution was passed through a cation exchanger resin in the Li^+ form (Dowex 50WX2). The resultant solution was evaporated to dryness, and the purity of the Li salts was checked by ^{1}H NMR in a D_2O-H_2O mixture.

Physical Methods. Analyses. Complete elemental analyses were performed by the Laboratoire Central d'Analyse du CNRS, Solaize, France. The water content was determined by thermal gravimetric analysis.

Infrared Spectra. IR spectra were recorded on an IRFT Magna 550 Nicolet spectrophotometer using the technique of pressed KBr pellets at a resolution of 0.5 cm^{-1}.

NMR Measurements. ^{1}H NMR spectra were recorded on a Brüker AC-300 spectrometer operating at 300.0 MHz in 5-mm tubes. ^{1}H chemical shifts were referenced to the external usual standard TMS.

Mass Spectrometry. The ESMS experiments were performed on a HP 5989B MS Engine. The tip of the capillary was at a potential of −3.5 kV, and the source temperature was 298 K. The mobile phase consists of a 75−25 mixture of water−methanol, and a flow rate of 10 μL min^{-1} was employed with a Harvard pump syringe. The cone voltage was −115 V relative to the skimmer. Mass spectra were acquired by scanning the quadrupole mass filter from *m*/*z* 1500 to 90, and approximately 50 scans were required to collect the mass spectrum.

Crystallography. Intensity data collection was carried out with a Siemens SMART three-circle diffractometer equipped with a CCD bidimensionnal detector using Mo Kα monochromatized radiation (λ = 0.71073 Å). An empirical absorption correction was applied (SADABS program[17] based on Blessing's methods[18]). The structures were solved by direct methods and refined by the full-matrix least-squares procedure (SHELX-TL package[19]). Crystals of $Cs_2[Mo_{12}\text{-pim}]\cdot 22H_2O$ rapidly lose water of crystallization, leading to an amorphous solid. Therefore, a single crystal of $Cs_2[Mo_{12}\text{-pim}]\cdot 22H_2O$ was mounted in a Lindemann tube (0.3 mm diameter). Relevant crystal data and data collection and refinement parameters for compounds $[NMe_4]_2[Mo_8\text{-ox}]\cdot 13H_2O$, $Cs_2[Mo_{10}\text{-}glu]\cdot 11H_2O$, $Rb_4glu[Mo_{10}\text{-}glu]\cdot 5H_2O$, and $Cs_2[Mo_{12}\text{-pim}]\cdot 22H_2O$ are summarized in Table 1. Heavy atoms for each structure were initially located by direct methods. The remaining non-hydrogen atoms were located from Fourier differences and were refined with anisotropic thermal parameters, except for the disordered atoms and water molecules.

$[N(CH_3)_4]_2[Mo_8S_8O_8(OH)_8(C_2O_4)]\cdot 13H_2O$, $[NMe_4]_2[Mo_8\text{-ox}]\cdot 13H_2O$. The central oxalate was found to be disordered over two positions in the ring. The resulting carbon atoms, C1 and C2, were refined isotropically with occupancy factors of $^1/_2$. The counterion $[NMe_4]^+$ is statistically distributed over two positions labeled A and B, respectively.

$Cs_2[Mo_{10}S_{10}O_{10}(OH)_{10}(C_5H_6O_4)]\cdot 11H_2O$, $Cs_2[Mo_{10}\text{-}glu]\cdot 11H_2O$. The three central carbon atoms of the encapsulated glutarate, namely C2, C3, and C4, were found to be distributed over two positions, giving the two enantiomeric conformations labeled C1−C2A−C3A−C4A−C5 and C1−C2B−C3B−C4B−C5, respectively. The electric balance was ensured by the two Cs1 and Cs2 atoms, which were statistically distributed over two positions labeled A and B, respectively.

$Rb_4(H_6C_5O_4)[Mo_{10}S_{10}O_{10}(OH)_{10}(H_6C_5O_4)]\cdot 5H_2O$, $Rb_4glu[Mo_{10}\text{-}glu]\cdot 5H_2O$. The inner glutarate adopts two enantiomeric conformations related through a mirror plane. One rubidium atom was found to be disordered over three positions. The occupancy factors were refined and subsequently fixed to 0.5, 0.3, and 0.2, respectively.

$Cs_2[Mo_{12}S_{12}O_{12}(OH)_{12}(H_{10}C_7O_4)]\cdot 22H_2O$, $Cs_2[Mo_{12}\text{-pim}]\cdot 22H_2O$. C4 (central carbon of the pimelate) is distributed over two disordered positions generated through the mirror plane containing the 12 Mo atoms of the ring. The $^1/_2$ cesium atom expected in the asymmetric unit is disordered over four positions. The occupancy factors of these crystallographic sites have been refined and finally constrained so that their sum has the expected value.

Acknowledgment. The authors thank Prof. Dr. A. Müller for allowing S.R. to work in Institut Lavoisier for a few months. Hervé Sayer from SIRCOB, Université de Versailles, is specially acknowledged for recording the ESMS spectra.

Supporting Information Available: Tables of positional and thermal parameters and estimated standard deviations for all atoms, bond distances, and angles and anisotropic thermal parameters for $[N(CH_3)_4]_2[Mo_8S_8O_8(OH)_8(C_2O_4)]\cdot 13H_2O$, $Cs_2[Mo_{10}S_{10}O_{10}(OH)_{10}(H_6C_5O_4)]\cdot 11H_2O$, $Rb_4(H_6C_5O_4)[Mo_{10}S_{10}O_{10}(OH)_{10}(H_6C_5O_4)]\cdot 5H_2O$, and $Cs_2[Mo_{12}S_{12}O_{12}(OH)_{12}(H_{10}C_7O_4)]\cdot 22H_2O$ (PDF). This material is available free of charge via the Internet at http://pubs.acs.org.

JA001878T

(17) Sheldrick, G. M. A program for the Siemens Area Detector ABSorption correction; University of Göttingen, Germany, 1997.

(18) Blessing, R. *Acta Crystallogr.* **1995**, *A51*, 33.

(19) Sheldrick, G. M. SHELX-TL version 5.03, Software Package for the Crystal Structure Determination Siemens Analytical X-ray Instruments Inc.; Madison, WI, 1994.